

# Polymerizable Vesicles Based on a Single-Tailed Fatty Acid Surfactant: A Simple Route to Robust Nanocontainers

Jae-Ho Lee,<sup>§,†</sup> Dganit Danino,<sup>‡</sup> and Srinivasa R. Raghavan<sup>\*,†</sup>

Department of Chemical & Biomolecular Engineering, University of Maryland, College Park, Maryland 20742-2111, and Department of Biotechnology and Food Engineering, Technion - Israel Institute of Technology, Technion, Haifa, Israel, 32000

Received July 23, 2008. Revised Manuscript Received November 11, 2008

Vesicles with polymerizable bilayers have attracted interest because of their increased robustness, which is advantageous for applications. However, to prepare such vesicles, lipids with polymerizable moieties usually need to be synthesized, and this often involves cumbersome, multistep reactions. Here, we present an alternative, simpler approach based on a commercially available, single-tailed surfactant, viz. 10-undecenoic acid (UDA), a fatty acid with a terminal double bond. Previously, the polymerization of UDA micelles in water has been studied. We show that UDA can also be induced to form vesicles by adjusting the pH: vesicles form at intermediate pH (6–8), whereas at higher pH (>11), the vesicles are transformed into micelles. The presence of UDA vesicles in the pH 6–8 range is confirmed using small-angle neutron scattering (SANS) and cryotransmission electron microscopy (cryo-TEM). Subsequent thermal polymerization of UDA bilayers is done using 2,2-dimethoxy-2-phenylacetophenone (DMPA) as initiator. A partial polymerization of the bilayers is achieved, and polymerized UDA vesicles resist disruption into micelles when the solution pH is increased. To make the bilayers more robust, the vesicles are copolymerized with divinylbenzene (DVB), a hydrophobic cross-linker that partitions into the bilayer. DVB-cross-linked UDA vesicles are very stable and cannot be disrupted by detergents like Triton X-100.

## 1. Introduction

A topic of great interest over the last two decades has been the creation of robust nanosized vesicles using polymerizable lipids.<sup>1–7</sup> The latter are lipids that bear some type of reactive group along their nonpolar tail(s), such as dienoyl, acryloyl, or lipoyl groups.<sup>4,5</sup> Vesicles (liposomes) formed from these lipids in aqueous solution can be subsequently polymerized by heat or UV light in the presence of a suitable initiator that generates free radicals. In the process, the tails in the vesicle bilayer become linked by strong, covalent bonds, and the vesicle is thereby converted into a robust nanocontainer.<sup>5,6</sup> Such polymerized vesicles cannot be destabilized by addition of bilayer-disrupting agents such as ethanol or Triton X-100 (unlike unpolymerized vesicles, which have low stability because they are self-assembled structures held only by weak, noncovalent bonds). Because of their increased stability, polymerizable vesicles have attracted much attention for applications, especially in drug, protein, or gene delivery.<sup>5,8</sup>

Despite decades of work, however, polymerizable vesicles have remained rather esoteric structures, and their technological potential has been underexploited. One reason has been the requirement of lipids with complex chemistries: the synthesis of such polymerizable lipids is often not a simple or cost-effective

process. Few such lipids are available commercially at present, and the ones that are available tend to be quite expensive. The present work arose out of our motivation to find a simpler approach to making robust vesicles with polymerized bilayers. In particular, we demonstrate the use of an inexpensive, commercially available fatty acid, 10-undecenoic acid (UDA), to make polymerizable vesicles.

It has been known for decades that two-tailed lipids are not the only kind of amphiphiles that can form vesicles; single-tailed surfactants can also do so under certain conditions.<sup>9–11</sup> Among such single-tailed surfactants are fatty acids, which represent a very basic type of amphiphile chemistry: an alkyl tail connected to a carboxylic acid group.<sup>10,11</sup> When added to water, fatty acids form micelles at high pH, which corresponds to full ionization of their carboxylic acid group. However, a lesser known aspect of fatty acid self-assembly is that they can form vesicles at intermediate pH values close to the  $pK_a$  of the molecule.<sup>10,11</sup> Vesicle formation by fatty acids has been of great interest to researchers involved in prebiotic chemistry, who have postulated the existence of fatty acids in the prebiotic soup of ancient earth (indeed, fatty acids have even been isolated from meteorites).<sup>12,13</sup> Accordingly, a number of researchers have constructed phase diagrams showing the type of aggregate as a function of pH for different fatty acids, including oleic acid, octanoic acid, and decanoic acid.<sup>14–16</sup>

\* Corresponding author. E-mail: sraghava@eng.umd.edu.

<sup>†</sup> University of Maryland.

<sup>‡</sup> Technion - Israel Institute of Technology.

<sup>§</sup> Present address: National Cancer Institute, Frederick, MD 21702.

(1) Regen, S. L.; Czech, B.; Singh, A. *J. Am. Chem. Soc.* **1980**, *102*, 6638.  
(2) Kunitake, T.; Okahata, Y.; Shimomura, M.; Yasunami, S. I.; Takarabe, K. *J. Am. Chem. Soc.* **1981**, *103*, 5401.

(3) Fendler, J. H. *Science* **1984**, *223*, 888.  
(4) Ringsdorf, H.; Schlarb, B.; Venzmer, J. *Angew. Chem., Int. Ed. Engl.* **1988**, *27*, 113.

(5) Mueller, A.; O'Brien, D. F. *Chem. Rev.* **2002**, *102*, 727.

(6) Liu, S. C.; O'Brien, D. F. *J. Am. Chem. Soc.* **2002**, *124*, 6037.

(7) Paul, G. K.; Indi, S. S.; Ramakrishnan, S. *J. Polym. Sci., Part A: Polym. Chem.* **2004**, *42*, 5271.

(8) Uchegbu, I. F. *Expert Opin. Drug Delivery* **2006**, *3*, 629.

(9) Kaler, E. W.; Murthy, A. K.; Rodriguez, B. E.; Zasadzinski, J. A. N. *Science* **1989**, *245*, 1371.

(10) Gebicki, J. M.; Hicks, M. *Nature* **1973**, *243*, 232.

(11) Hargreaves, W. R.; Deamer, D. W. *Biochemistry* **1978**, *17*, 3759.

(12) Deamer, D. W. *Microbiol. Mol. Biol. Rev.* **1997**, *61*, 239.

(13) Szostak, J. W.; Bartel, D. P.; Luisi, P. L. *Nature* **2001**, *409*, 387.

(14) Cistola, D. P.; Hamilton, J. A.; Jackson, D.; Small, D. M. *Biochemistry* **1988**, *27*, 1881.

(15) Apel, C. L.; Deamer, D. W.; Mautner, M. N. *Biochim. Biophys. Acta* **2002**, *1559*, 1.

(16) Morigaki, K.; Walde, P.; Misran, M.; Robinson, B. H. *Colloids Surf. A* **2003**, *213*, 37.

One fatty acid for which vesicle formation has *not* been studied to our knowledge is UDA. However, micelles of UDA (at high pH) have been studied extensively since the 1980s.<sup>17–19</sup> Structurally, the unique characteristic of UDA is the presence of a terminal double bond on its alkyl tail. Accordingly, many investigators have sought to polymerize UDA micelles, and the feasibility of such polymerization has been demonstrated under specific conditions.<sup>20–26</sup> These previous studies suggested to us that if UDA vesicles could indeed be formed, they could also be polymerized. We have therefore investigated the self-assembly of UDA as a function of pH, and we have proceeded to construct a phase diagram for UDA, much like for other fatty acids. Vesicles are indeed found at intermediate pH, and we confirm their presence using small-angle neutron scattering (SANS) and cryotransmission electron microscopy (cryo-TEM). We then study the polymerization of UDA vesicles using conditions that have been used before for polymerization of UDA micelles. To further improve the robustness of these vesicles, we copolymerize UDA vesicles in the presence of a hydrophobic monomer (divinylbenzene, DVB).<sup>26–28</sup> Our results indicate that UDA polymerization can provide a simple route toward robust nanocontainers. It is tempting to speculate whether polymerizable fatty acid vesicles could perhaps be relevant even to the creation of confined environments in prebiotic times.

## 2. Experimental Section

**2.1. Materials.** The anionic fatty acid UDA (>98%), the initiators benzophenone (BP) and 2,2-dimethoxy-2-phenylacetophenone (DMPA), the monomer DVB, and bicine and HEPES buffers were all purchased from Sigma-Aldrich. The nonionic detergent, Triton X-100 (chemical name: 4-octylphenol polyethoxylate; average 9.5 ethylene oxide units), which is a known vesicle destabilizing agent, was also obtained from Sigma-Aldrich. D<sub>2</sub>O (99.5% D) for the SANS experiments was obtained from Cambridge Isotopes.

**2.2. Vesicle Formation.** UDA vesicles were prepared by adding UDA to deionized water and adjusting the pH of the solution. Typically, UDA vesicles were made in a 0.2 M bicine buffer solution, with the pH controlled by addition of NaOH. The titration curve for UDA as a function of pH was done using concentrated HCl and is described in detail in Results.

**2.3. Vesicle Polymerization.** UDA vesicles were polymerized in one of two ways, which are described in more detail in Results. In the first case, DMPA initiator and UDA were combined, and this mixture was used to form UDA vesicles in buffer, as described above. The vesicles were then polymerized by heating the solution to 70 °C for 48 h. In the second case, the monomer DVB and the initiator BP were combined with UDA (typical composition, 100 parts UDA/5 parts DVB/0.25 parts BP). This mixture was used to form UDA vesicles, with the DVB partitioning into the hydrophobic bilayer. The vesicles were then polymerized by UV

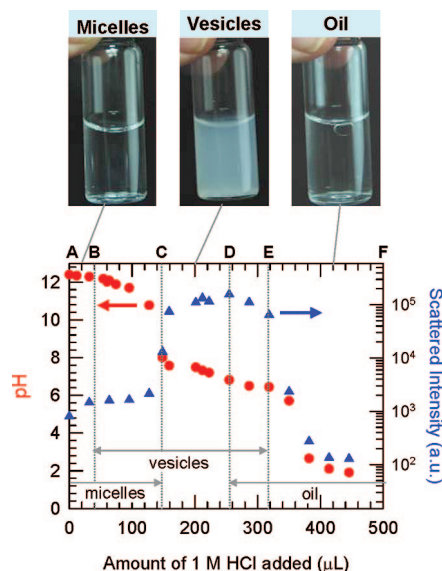


**Figure 1.** Titration curve for 2% UDA at room temperature. Varying amounts of 1 M HCl were added to a micellar solution of UDA (pH 12). After the samples reached equilibrium, the pH and the intensity of scattered light (arbitrary units) were recorded and are shown on the plot. Photographs of selected samples are also shown.

light (365 nm) for 2 h using a Oriel 200 W mercury arc lamp. Polymerization-induced chemical changes were analyzed by Fourier-transform infrared spectroscopy (FTIR) using a Nicolet 5DXC spectrometer.

**2.4. Dynamic Light Scattering (DLS).** Vesicle solutions were studied at 25 °C using DLS. A Photocor-FC light scattering instrument with a 5 mW laser light source at 633 nm was used, with the scattering angle being 90°. A logarithmic correlator was used to obtain the autocorrelation function, from which a diffusion coefficient was extracted. The apparent hydrodynamic size of the vesicles was obtained from the diffusion coefficient through the Stokes–Einstein relationship.

**2.5. Small Angle Neutron Scattering (SANS).** SANS measurements were made on the NG-3 (30 m) and NG-1 (8 m) beamlines at NIST in Gaithersburg, MD. Samples were studied at 25 °C in 2 mm quartz cells. The scattering spectra were corrected and placed on an absolute scale using calibration standards provided by NIST. SANS data are shown as plots of the radially averaged absolute intensity  $I$  vs the wave vector  $q = (4\pi/\lambda)\sin(\theta/2)$ , where  $\lambda$  is the wavelength of incident neutrons and  $\theta$  the scattering angle.

**2.6. Cryo-TEM.** Samples for cryo-TEM were prepared in a controlled environment vitrification system (CEVS).<sup>29</sup> In the CEVS, samples were quenched rapidly into liquid ethane at its freezing point of −183 °C, so as to form vitrified specimens. The samples were then transferred to liquid nitrogen for storage and thereafter examined on a Philips CM120 microscope operated at 120 kV, with an Oxford CT-3500 cryoholder used to maintain the samples below −180 °C. Digital images were recorded in the minimal electron dose mode by a Gatan 791 MultiScan cooled CCD camera.<sup>29</sup>

## 3. Results and Discussion

**3.1. UDA Titration Curve and Vesicle Window.** First, we present the equilibrium titration curve as a function of pH for UDA in Figure 1. Such titration curves have been reported

(17) Sprague, E. D.; Duecker, D. C.; Larrabee, C. E. *J. Colloid Interface Sci.* **1983**, 92, 416.

(18) Larrabee, C. E.; Sprague, E. D. *J. Colloid Interface Sci.* **1986**, 114, 256.

(19) Rodriguez, J. L.; Schulz, P. C.; Puig, J. E. *Colloid Polym. Sci.* **1999**, 277, 1072.

(20) Larrabee, C. E.; Sprague, E. D. *J. Polym. Sci. C* **1979**, 17, 749.

(21) Denton, J. M.; Duecker, D. C.; Sprague, E. D. *J. Phys. Chem.* **1993**, 97, 756.

(22) Paleos, C. M.; Stassinopoulou, C. I.; Malliaris, A. *J. Phys. Chem.* **1983**, 87, 251.

(23) Chu, D. Y.; Thomas, J. K. *Macromolecules* **1991**, 24, 2212.

(24) Durairaj, B.; Blum, F. D. *Langmuir* **1989**, 5, 370.

(25) Arai, K.; Sugita, J.; Ogiwara, Y. *Makromol. Chem.-Macromol. Chem. Phys.* **1987**, 188, 2511.

(26) Arai, K. *Makromol. Chem.* **1993**, 194, 1975.

(27) McKelvey, C. A.; Kaler, E. W.; Zasadzinski, J. A.; Coldren, B.; Jung, H. T. *Langmuir* **2000**, 16, 8285.

(28) Hubert, D. H. W.; Jung, M.; German, A. L. *Adv. Mater.* **2000**, 12, 1291.

(29) Danino, D.; Bernheim-Groswasser, A.; Talmon, Y. *Colloid Surf. A* **2001**, 183, 113.

previously for other fatty acids such as oleic ( $C_{18}$ ) and decanoic acid ( $C_{10}$ ),<sup>11,14,16</sup> the progression generally being from micelles at high pH (9–12) to vesicles at moderate pH near the  $pK_a$  of the fatty acid (pH ca. 6–9) and finally to droplets of the insoluble fatty acid (“oil”) at lower pH. Similar results are found in the present case as well. Our experiments were done for 2 wt% UDA (i.e., 110 mM) at 25 °C. Note that this concentration is higher than the reported CMC of UDA, which is 100 mM. We began with a solution of 2% UDA at a pH of about 12, and to this we added successive amounts of concentrated HCl. Each solution was kept for at least 3 days at room temperature, following which we analyzed the sample using DLS. Figure 1 shows the scattered intensity (a measure of turbidity) as well as the solution pH as a function of added HCl.

Consider the results of Figure 1, starting from high pH (added HCl = 0). At high pH, UDA is fully ionized and the UDA headgroups thus bear a strong negative charge. The repulsions of these headgroups leads to the formation of spherical micelles. Because the micelle size is only around 4 nm, a low scattered intensity is measured by DLS. As seen in the photograph, these micellar solutions are clear and colorless. This scenario persists for low amounts of HCl, and the solution pH stays around 12 (interval AB on the plot). Next, over interval BC (40 to 150  $\mu$ L HCl), the solution pH drops considerably and there is a modest increase in the scattered intensity. In this region a small proportion of the micelles are transformed into vesicles, and the two structures coexist in solution. The next interval, CD (150 to 250  $\mu$ L HCl) is the main region of interest. Over this interval, the pH is approximately constant around 7. The scattered intensity is high, a particle diameter  $\sim$  20 nm is measured, and the samples are homogeneous and have a strong bluish color (see photograph). These samples contain mostly vesicles, as will be further confirmed by SANS. At higher HCl amounts (interval DE, 250 to 320  $\mu$ L), oily droplets begin to form in the bluish samples. Finally, above 320  $\mu$ L of HCl, the pH plummets, the samples lose their bluish tinge, and oily droplets (of undissociated fatty acid) float at the top of the water (see photograph).

The above titration curve indicates that, at 2 wt%, UDA forms vesicles over a pH range of 6.7 to 8.0 (this is the “vesicle window”). In this regard, UDA behaves much like other fatty acids.<sup>14–16</sup> There is a question regarding the precise value of the  $pK_a$  of UDA. While a previous estimate of 5.4 has been reported for the  $pK_a$ ,<sup>19</sup> it is known that fatty acids can show a shift in their  $pK_a$  to a higher value.<sup>11,14,16</sup> Such shifts occur because protons are locally confined between fatty acid molecules and are thereby depleted in the bulk. For UDA, the apparent  $pK_a$  from the midpoint of the equilibrium titration curve between B and E is 7.5. Using this apparent value, the ratio of ionized to un-ionized UDA molecules is ca. 3.2 at C and 0.2 at D, which represent the limits for vesicle formation. The  $pK_a$  itself corresponds to a 1:1 ratio between the ionized and un-ionized species: this is an idealized scenario for vesicle formation, where a proton is shared between exactly two adjacent UDA molecules (some researchers have interpreted this process as the formation of fatty acid dimers<sup>11,14</sup>). More generally, one can consider the vesicles to be extended aggregates, stabilized both by proton sharing between fatty acid headgroups and by hydrophobic interactions between the fatty acid tails.

We have also determined the pH range for vesicle formation (i.e., “vesicle window”) at other UDA concentrations (data not shown). Interestingly, vesicles could be formed even at 1 wt% UDA, which is lower than the CMC. At this concentration, vesicles were only formed over a narrower pH range: between 6.7 and 7.2. Indeed, other researchers have also reported that

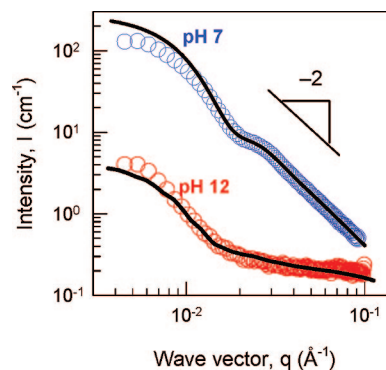


**Figure 2.** SANS data for 2% UDA solutions at pH 7 and pH 12. Model fits to the data are shown as solid lines (see text for details).

fatty acids can form vesicles below their CMCs; in most cases, the onset of vesicle formation occurs at approximately half the CMC.<sup>11,14</sup> Also, vesicles are not formed at very high fatty acid concentrations, above 6 wt% in the case of UDA. At these higher concentrations, a viscous, inhomogeneous mixture is instead produced, which corresponds to coexistence between a lamellar phase and a micellar solution. We also studied the effect of temperature on the vesicle window by conducting experiments at 70 °C. At 2 wt%, the vesicle window at 70 °C spanned a pH range of 6.7 to 7.7, which is slightly narrower than that at 25 °C. A similar result has been reported for dodecanoic acid vesicles.<sup>11</sup> The key point from the temperature study was that UDA vesicles at a pH around 7 remained stable upon heating (their diameter from DLS was also invariant with temperature). This allows the polymerization of the vesicles by heat (as will be discussed presently).

### 3.2. UDA Vesicle Characterization by SANS and Cryo-TEM.

We also obtained independent confirmation for the presence of UDA vesicles using SANS and cryo-TEM. For SANS studies, UDA solutions were prepared in  $D_2O$  to achieve the needed contrast between the microstructure and the solvent. Figure 2 shows SANS spectra for 2 wt% UDA solutions at pH 7 and pH 12. At pH 7, the scattered intensity  $I(q)$  exhibits a  $q^{-2}$  decay at moderate  $q$ , which is characteristic of bilayer scattering.<sup>30–32</sup> A model for polydisperse unilamellar vesicles<sup>32</sup> can be applied to this data, and the fit is shown as a solid line. From the model fit, the vesicles are estimated to have an average diameter of 26 nm with 30% polydispersity. The bilayer thickness is found to be  $1.7 \pm 0.5$  nm (independently confirmed in a model-free manner by a cross-sectional Guinier plot of the data<sup>32</sup>). For comparison, the extended length of a single  $C_{11}$  tail in UDA is estimated to be about 1.3 nm (using the Tanford formulas<sup>33</sup>). The estimated bilayer thickness is thus much less than twice the extended length of a UDA tail, which suggests that either the tails in UDA bilayers are considerably compressed<sup>34</sup> or there is intercalation of UDA tails from the two bilayer leaflets.

SANS data in Figure 2 for the same UDA solution at pH 12 shows striking differences from that at pH 7. The intensity at pH 12 is reduced by 2 orders of magnitude at low  $q$ . There is no interaction peak; however, there is an upturn at low to moderate

(30) Zemb, T.; Lindner, P., Eds. *Neutron, X-Ray and Light Scattering: Introduction to an Investigative Tool for Colloidal and Polymeric Systems*; Elsevier: Amsterdam, 1991.

(31) Pedersen, J. S. *Adv. Colloid Interface Sci.* **1997**, 70, 171.

(32) Lee, J. H.; Gustin, J. P.; Chen, T. H.; Payne, G. F.; Raghavan, S. R. *Langmuir* **2005**, 21, 26.

(33) Evans, D. F.; Wennerstrom, H. *The Colloidal Domain: Where Physics, Chemistry, Biology, and Technology Meet*; Wiley-VCH: New York, 2001.

(34) Namani, T.; Ishikawa, T.; Morigaki, K.; Walde, P. *Colloid Surf., B* **2007**, 54, 118.



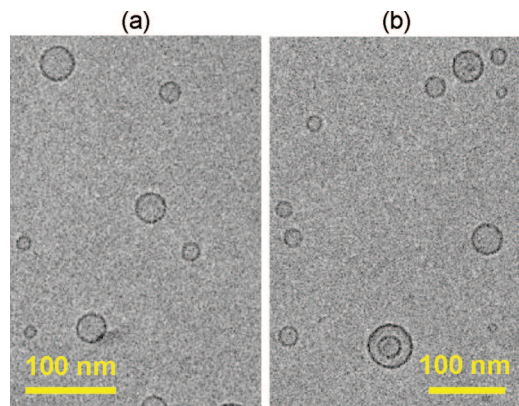


**Figure 3.** Cryo-TEM images of 1 wt% UDA vesicles in pH 7 buffer. A number of small unilamellar vesicles are seen.

*q*. We have modeled this sample as being a combination of spherical micelles and a small population of unilamellar vesicles with the same size as above (details in Supporting Information).<sup>36</sup> From the model fit, the fraction of surfactant in micelles was 99% and the micelle radius was found to be 1.5 nm. In other words, the vesicles being larger than the micelles still contribute substantially to the low-*q* scattering even though their number density is low. The coexistence of micelles with a small amount of vesicles at this pH is broadly consistent with our titration curve (Figure 1) and with studies on other fatty acids.<sup>14,16</sup> Incidentally, despite being mixtures of structures, samples around pH 12 remain as homogeneous solutions for months.

SANS data were also acquired at other solution pH (data not shown), and the results were quite consistent. At a pH of 8, the data is vesicle-like, similar to that at pH 7. However, at a pH of 8.5, the intensity drops significantly and the data are practically identical to the pH 12 scattering curve (indicating that most of the vesicles are disrupted into micelles). A similar drop in scattered intensity from pH 8 to 8.5 was also seen by DLS and is indicated in the titration curve (Figure 1). In other words, SANS is able to track the changes in the titration curve.

SANS data were additionally acquired at other UDA concentrations (data not shown). Scattering data characteristic of vesicles was found for 1, 2, and 4 wt% UDA solutions at pH 7. From fits to the vesicle model,<sup>32</sup> the average vesicle diameter was found to increase with concentration: from 20 nm (1%) to 26 nm (2%) to 98 nm (4%) while the bilayer thickness remained the same in all cases ( $1.7 \pm 0.5$  nm). A similar size increase was also observed for these vesicles by DLS. The vesicle sizes found here are quite comparable to those reported for other fatty acid vesicles.<sup>34,35</sup>

Cryo-TEM was also conducted on UDA solutions to further substantiate the presence of vesicles. Figure 3 shows cryo-TEM images of a 1% UDA solution at pH 7. A polydisperse population of unilamellar vesicles is seen, most of them smaller than 50 nm. This is in broad agreement with our SANS modeling and with cryo-TEM studies on other fatty acid vesicles.<sup>34,35</sup> A few multilamellar vesicles (typically with two lamellae) were occasionally found in the images; an example can be seen in Figure 3b. In summary, we have amassed evidence from a number of techniques, including DLS, SANS, and cryo-TEM, to indicate that UDA, much like other fatty acids, forms vesicles over an intermediate pH range.

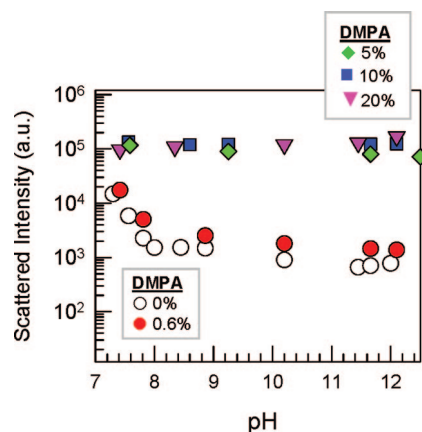


**Figure 4.** Stability test (response to pH spike) on 1% UDA vesicles polymerized by heat using varying amounts of DMPA initiator (the numbers correspond to wt% relative to the UDA). The control, unpolymerized vesicles (0% DMPA) are disrupted into micelles as the pH is raised, causing a sharp drop in the scattered intensity. In contrast, polymerized UDA vesicles (5% DMPA or more) are stable to the pH change, i.e., there is no loss in intensity with increasing pH.

**3.3. UDA Vesicle Polymerization.** Having demonstrated the presence of stable unilamellar UDA vesicles at a pH around 7, we proceeded to attempt polymerization of their vesicle bilayers. Previously, partial polymerization of UDA micelles has been achieved using reactive free-radical initiators.<sup>20–26</sup> The choice of initiator and the initiator concentration relative to UDA are important variables; here we chose DMPA as the initiator, and we studied a range of DMPA concentrations. Note that DMPA is a thermal initiator that dissociates to form free radicals at high temperatures. UDA vesicles (1 wt% concentration) were polymerized in the presence of DMPA for 24 h at 70 °C. Following thermal polymerization, the samples were stored at room temperature and then tested for vesicle stability.

A convenient test of vesicle stability involved subjecting the vesicles to a pH spike. From the titration curve, it is clear that a spike from pH 7 to 12 induces unpolymerized vesicles to break apart and transform into micelles; this process is rapid and completed within seconds.<sup>16</sup> To test the pH response, we added a solution of 5% NaOH dropwise into the vesicle solution (initially at pH 7) and recorded the change in scattered intensity by DLS. The results are presented in Figure 4. For the control, i.e., unpolymerized UDA vesicles (unfilled symbols) the trend is as expected: the intensity rapidly drops off with increasing pH and saturates at a low value (visually the sample goes from bluish to colorless). This indicates that the unpolymerized vesicles are converted into micelles. Polymerized UDA vesicles, in contrast, show a different behavior (filled symbols in Figure 4). A pH spike from 7 to 12 has no effect on the scattering intensity (i.e., the samples remain strongly bluish), and the vesicle diameter from DLS is also unchanged. This implies that polymerized vesicles are stable to changes in pH, evidently because many of the tails in each vesicle bilayer are now connected by covalent bonds. Note that if the DMPA used was too low (e.g., only 0.6% of the UDA concentration), the vesicles do not get polymerized and consequently they do fall apart at high pH (Figure 4). The DMPA used must be at least 5% of the UDA for sufficient polymerization to occur.

While polymerization of 1% UDA vesicles yields somewhat robust structures, similar polymerization of vesicles at 2% or higher UDA concentrations did not produce analogous results; i.e., those vesicles were not stable to a pH spike. Generally, the yields from free-radical polymerization of  $\alpha$ -olefins are low

(35) Berclaz, N.; Blochliker, E.; Muller, M.; Luisi, P. L. *J. Phys. Chem. B* **2001**, *105*, 1065.

(36) Hjelm, R. P.; Schteingart, C. D.; Hofmann, A. F.; Thiyagarajan, P. *J. Phys. Chem. B* **2000**, *104*, 197.

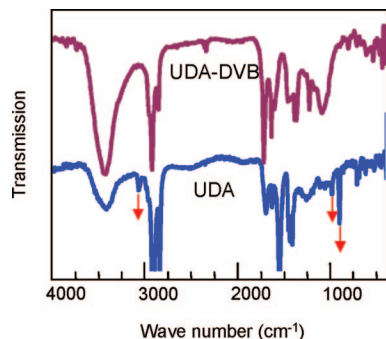


**Figure 5.** FTIR spectra for UDA and polymerized UDA-DVB. The red arrows indicate peaks corresponding to the terminal double bond in UDA. These peaks are absent in the spectrum after polymerization.

because of autoinhibition by the allylic hydrogens.<sup>37</sup> Indeed, prior attempts at polymerizing UDA micelles only produced oligomers ( $\sim 10$ -mers).<sup>20–26</sup> For the case of UDA vesicles, in addition to DMPA-initiated thermal polymerization, we have also tried UV and  $\gamma$ -ray polymerization and also a variety of other initiators. In all cases, we were unable to get vesicles that could resist disruption at high pH. Moreover, while the thermally polymerized 1% UDA were resistant to pH changes, they could still be disrupted by stronger destabilizing agents such as the detergent Triton X-100. In other words, direct polymerization of UDA vesicles can only be done to a limited extent, and an alternative approach is therefore necessary.

### 3.4. UDA Vesicle Polymerization in the Presence of DVB.

We therefore investigated the use of a cross-linking monomer, DVB. This strategy is similar to the one that has been used by others,<sup>26–28</sup> (see review by German et al.<sup>28</sup>). The idea is to copolymerize the DVB with the double bonds on UDA so as to yield a robust bilayer in which all the tails are linked together. Toward this end, we combined 1% UDA vesicles with 0.05 wt% DVB and a small amount of BP initiator. The DVB and BP, being hydrophobic, partitioned into the UDA vesicle bilayers without affecting the integrity of the vesicles. The sample was then polymerized by UV light (thermal polymerization also works). To confirm that the double bonds on UDA react with the DVB, we used FTIR. Figure 5 shows FTIR spectra before and after polymerization. The peaks corresponding to UDA double bonds, i.e.,  $3080\text{ cm}^{-1}$  and  $1640\text{ cm}^{-1}$  ( $\text{C}=\text{C}$  stretch),  $990\text{ cm}^{-1}$  ( $\text{C}=\text{C}$  out of plane bend), and  $910\text{ cm}^{-1}$  ( $\text{C}-\text{H}$  out of plane bend for the  $=\text{CH}_2$ ) are no longer present after polymerization, indicating that copolymerization does occur. Similar polymerization with DVB was also done at other UDA vesicle concentrations from 2 to 6 wt%. We should point out that instead of BP, other initiators such as azobis(isobutyronitrile) (AIBN) or DMPA can also be used, and the polymerization can also be done by heat instead of UV.

We then proceeded to evaluate the robustness of UDA-DVB vesicles. This was done in two ways, first by subjecting the vesicles to a pH spike, and second by addition of Triton X-100. The UDA-DVB vesicles proved to be stable to both these perturbations. As mentioned before, the Triton X-100 test is the more stringent one, and the corresponding results are shown in Figure 6. Before polymerization, UDA vesicles break apart when about 15 mM of Triton X-100 is added; this is seen by the rapid decrease in the scattered intensity for this case. In contrast, polymerized UDA vesicles remain stable regardless of the Triton X-100 concentration (no loss in scattered intensity). The average diameter of the vesicles after polymerization (about 109 nm)

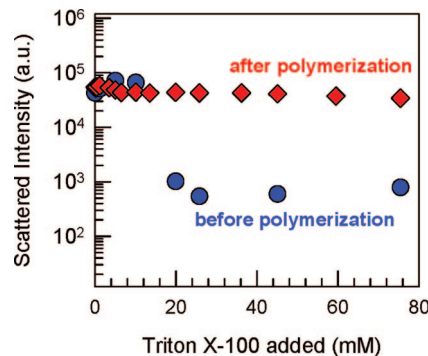


**Figure 6.** Stability test using the nonionic detergent, Triton X-100, on 1% UDA vesicles copolymerized with DVB. Unpolymerized vesicles break apart into micelles upon detergent addition, resulting in a loss of scattered intensity. On the other hand, polymerized vesicles are very stable to detergent addition and show no decrease in scattered intensity.

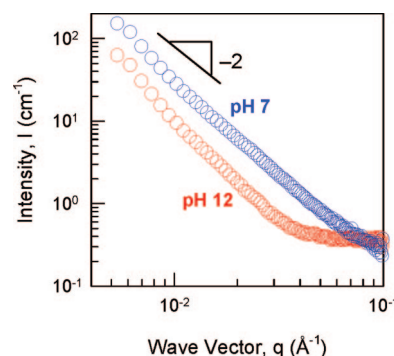


**Figure 7.** SANS data for DVB-polymerized 1% UDA solutions at pH 7 and pH 12. The data show a slope close to  $-2$  in both cases. The weak effect of pH on the SANS data reflects the increased stability of the polymerized vesicles.

was also insensitive to the addition of Triton X-100. Analogous results were also found when the polymerized vesicles were subjected to a pH spike (data not shown).

We also conducted SANS studies on polymerized UDA-DVB vesicles as a function of pH. The SANS scattered intensity  $I(q)$  shows a  $q^{-2}$  decay at moderate  $q$  for both pH 7 and 12 (Figure 7). The  $q^{-2}$  decay shows that the vesicle structure is retained after polymerization (with the polymerization taking place uniformly across the bilayer).<sup>27</sup> When the pH is raised to 12, there is a small drop in the intensity at low  $q$ , while the plateau at higher  $q$  indicates scattering from spherical micelles. In other words, there is a small fraction of UDA vesicles that are not fully polymerized, and these get disrupted into micelles when the pH is increased. Modeling the SANS data from the polymerized vesicle sample gives an average vesicle diameter of  $\sim 112\text{ nm}$  and  $3.7 \pm 0.5\text{ nm}$  for the bilayer thickness. Compared to their values before polymerization (diameter  $\sim 26\text{ nm}$ , bilayer thickness  $1.7 \pm 0.5\text{ nm}$ ), both parameters are significantly increased. The higher value of the bilayer thickness in this case was again confirmed in a model-free manner using cross-sectional Guinier plots (see Supporting Information for an example). The increase in bilayer thickness may imply that the tails in the polymerized bilayer are in a fully extended conformation. Alternately, the increased thickness may reflect the presence of “dimpled” vesicles as seen in the cryo-TEM images below. Likewise, the increase in the average diameter is probably due to the presence of some aggregated vesicle structures, as also revealed below by cryo-TEM.

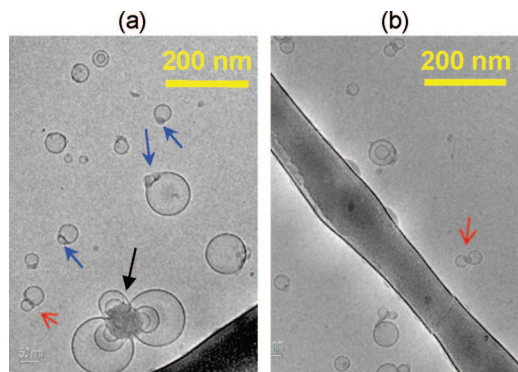


**Figure 8.** Cryo-TEM images of DVB-polymerized 1% UDA vesicles. Specific structures of interest in the images are indicated by colored arrows (see text for details).

Cryo-TEM images are shown in Figure 8 for polymerized UDA–DVB vesicles. The images show several interesting aspects. First, a number of small, unilamellar vesicular structures are seen (of a size comparable to those in Figure 3). These structures generally have a “dimple” at one end (blue arrows) but otherwise seem identical to their unpolymerized counterparts. We believe that the dimpled unilamellar structures are a mostly accurate template of the original vesicles. German et al.<sup>28,38</sup> have shown that the polymerization of a monomer in the bilayer leads to phase separation of the resulting polymer and consequently to the formation of “parachute” structures, in which the vesicle shape is considerably distorted. The same group also demonstrated a way to prevent parachute formation, which is to use vesicles made from a polymerizable lipid.<sup>39</sup> The latter result is relevant here, since UDA in the bilayer is capable of being copolymerized with DVB chains. The dimples likely represent the onset of polymer phase separation, but this is curtailed because of the ability of the UDA to react with the growing DVB network within the bilayer. Note that the added thickness of the dimpled regions may partially account for the higher bilayer thickness obtained from SANS modeling.

Figure 8 also shows several doublets, i.e., two vesicles coming into close contact (red arrows) and a few large multilamellar aggregates (black arrow). The latter are a very small component of the overall population, although they probably contribute to

the increase in size observed by DLS as a result of polymerization. With regard to the doublets, they may represent a fusion of two vesicles due to polymerization at their interface. Nevertheless, based on both SANS and cryo-TEM, the majority of UDA vesicles do seem to undergo a uniform controlled polymerization together with the DVB in the bilayer. The unilamellar vesicle structure is largely retained, with the slope in SANS remaining close to  $-2$ . Thus, polymerization of UDA vesicles assisted by DVB is certainly feasible, and it is clear that the polymerized structures are very robust, being able to resist disruption by both Triton X-100 and a pH spike. Because the vesicle-forming surfactant is linked to the polymer, purification of the resulting hollow spheres is also quite straightforward. The same procedure should also work with a variety of other cross-linkable hydrophobic monomers.

#### 4. Conclusions

We have shown in this paper that UDA, a single-tailed fatty acid with a terminal unsaturation on its alkyl tail, is capable of forming unilamellar vesicles over an intermediate range of pH (6–8). The presence of vesicles was demonstrated by a variety of techniques, including DLS, SANS, and cryo-TEM. When the pH of the solution is increased to  $>10$ , UDA vesicles break up into micelles, which is reflected as a sharp decrease in the intensity of light scattered from the sample. We sought to polymerize UDA vesicles directly using DMPA as the initiator. Polymerized 1% UDA vesicles could not be disrupted into micelles by increasing pH; however, they could be destabilized by addition of Triton X-100. To confer additional stability, we copolymerized the vesicle bilayers with DVB, a hydrophobic cross-linker. In the process, the DVB molecules connected UDA chains to form a robust bilayer. DVB-cross-linked UDA vesicles were very stable and could not be disrupted even by Triton X-100. Cryo-TEM and SANS were used to confirm that vesicle polymerization occurred with retention of structure.

**Acknowledgment.** This work was partially funded by a seed grant from the NSF-funded MRSEC at UMD. We acknowledge NIST NCNR for facilitating the SANS experiments performed as part of this work. D.D. acknowledges equipment grants from the ISF and from RBNI.

**Supporting Information Available:** More details of SANS modeling in Figures 2 and 7. This information is available free of charge via the Internet at <http://pubs.acs.org>.

LA802373J

(38) Jung, M.; Hubert, D. H. W.; van Veldhoven, E.; Frederik, P.; van Herk, A. M.; German, A. L. *Langmuir* **2000**, *16*, 3165.

(39) Jung, M.; den Ouden, I.; Montoya-Goni, A.; Hubert, D. H. W.; Frederik, P. M.; van Herk, A. M.; German, A. L. *Langmuir* **2000**, *16*, 4185.



## Supporting Information for

### Polymerizable Vesicles Based on a Single-Tailed Fatty Acid Surfactant: A Simple Route to Robust Nano-Containers

*Jae-Ho Lee, Dganit Danino & Srinivasa R. Raghavan\**

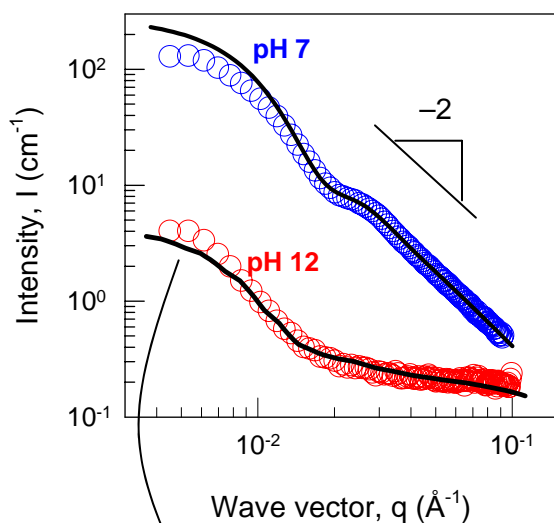
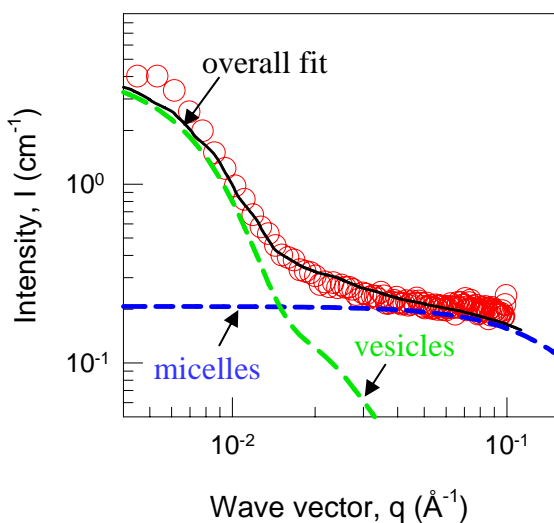


**Figure 2.** SANS data for 2% UDA solutions at pH 7 and pH 12. Model fits to the data are shown as solid lines (see text for details).

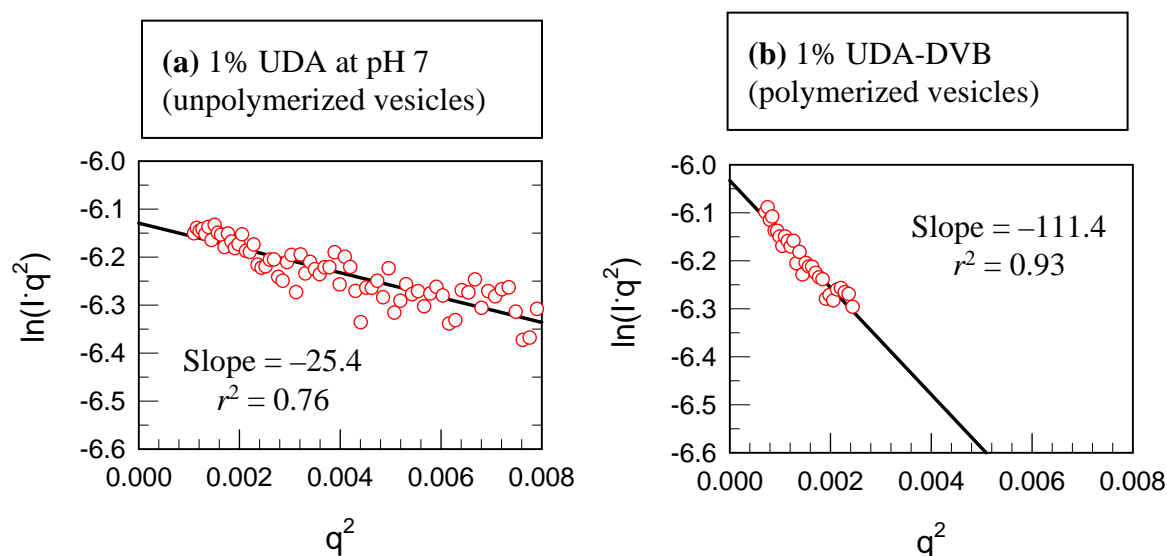
pH 12 data modeled as mixtures of vesicles + spherical micelles, as detailed in Figure S1 below.



$$I_{\text{overall}}(q) = c [\phi_m P_{\text{micelle}}(q) + (1 - \phi_m) P_{\text{vesicle}}(q)]$$

Here  $c$  is the overall concentration and  $\phi_m$  is the volume fraction of spherical micelles.  $P_{\text{micelle}}(q)$  and  $P_{\text{vesicle}}(q)$  are the respective form factors, expressions for which are given in Refs. 30-32. From the model fit, we find  $\phi_m = 0.99$ , i.e., the sample is a mixture of 99% micelles and 1% vesicles (see text for more details).

**Figure S1**



$$\text{Bilayer thickness, } t = \sqrt{|slope| \times 12}$$

**Figure S2.** Cross-sectional Guinier plots of the SANS data for (a) 1% UDA (unpolymerized) and (b) 1% UDA-DVB (polymerized) vesicles. The data are shown over the same x and y scales to indicate the significantly higher slope for the latter. The slope yields the bilayer thickness via the equation shown. From the values here, we find  $t = 1.7$  nm for (a) and  $t = 3.7$  nm for (b).

Ref: Kucerka, N.; Kiselev, M. A.; Balgavy, P., "Determination of bilayer thickness and lipid surface area in unilamellar dimyristoylphosphatidylcholine vesicles from SANS curves: A comparison of evaluation methods." *Eur. Biophys. J.* **2004**, 33, 328.